Induced Unilateral Vocal Fold Paralysis and Recovery Rapidly Modulate Brain Areas Related to Phonatory Behavior: A Case Study

***Ashwini Joshi, †Yang Jiang, *Joseph C. Stemple, ‡Sanford M. Archer, and *Richard D. Andreatta,** *†‡*Lexington, Kentucky*

Summary: Background. Peripheral and behavioral effects of voice disorders are well documented in the literature; yet, there is little information regarding the central neural biomarkers and mechanisms underlying these disorders. Understanding the details of brain function changes in disordered voice production is a critical factor for developing better treatment strategies that result in more robust patient outcomes.

Objective. To examine a model of induced unilateral vocal fold paralysis (iUVFP) to demonstrate and characterize the form of activity changes within central mappings of the larynx to the induced paralysis. The induced paralysis model allowed the participant to serve as his or her own control when comparing baseline results of normal voice with results during the paralysis and subsequent recovery.

Study Design. Prospective, case-study design.

Methods. Functional magnetic resonance imaging was used to examine central laryngeal representations during three time points: pre-iUVFP, during iUVFP, and postrecovery from iUVFP. iUVFP was induced using a lidocaine with epinephrine nerve block unilaterally. Percent changes in blood oxygenation level-dependent (BOLD) activity served as the dependent variable.

Results. Results indicated an overall reduced activity level in sensorimotor, subcortical, and cerebellar regions during paralysis. Recovery from paralysis led to augmented responses, particularly in sensory, association, and cerebellar zones.

Conclusions. The decrease in activity during iUVFP and the significantly increased activity during the recovery phase likely represent immediate neuroplastic events occurring within minutes of nerve blockade. Recovery-related changes in the BOLD response are hypothesized to be associated with a recalibration of the system after return of normal laryngeal function.

Key Words: Vocalization—Neuroplasticity—Voice disorder—Nerve block—Reorganization.

INTRODUCTION

Although much is known about the peripheral effects of voice disorders, little is understood of the relationship between behavioral features of voice disorders and the consequences of these features on central neural mappings. Because speech and language are uniquely human, the existing animal models are inherently limited in their capacity to represent human speech and skilled vocal performance. Methodological advancements in noninvasive neuroimaging techniques, such as functional magnetic resonance imaging (fMRI) and sparse sampling designs, are readily available and useful for overcoming significant artifactual obstacles in the study of production variables related to speech and voice.[1–4] As a result, data are now emerging on the characteristics of central representations of the larynx during human voice production and running speech. For example, studies by Haslinger et al,[1] Ozdemir et al,[4] Loucks et al,[3] and Huang et al[2] have all identified core brain regions activated during normal speech and voice tasks. These areas include, but are not limited to, the primary sensory and motor areas, anterior cingulate cortex, midline cerebellum, thalamus, and the periaqueductal gray region among others.

Few reports using neuroimaging techniques are available for those with disordered voice compared with normal vocal abilities. Of the work currently available on disordered voice populations, there is one report in persons with Parkinson disease[5] and another in spasmodic dysphonia[6] using positron emission tomography. fMRI[7] and diffusion tensor imaging[8] have also been used to study persons with spasmodic dysphonia, and a more recent case study was performed in a person with an acquired unilateral vocal fold paralysis (UVFP) using fMRI.[9]

The observed deleterious effects in voice quality and production consequent to disease and injury described in these studies demonstrate the value for understanding the central neural representation of the laryngeal system in both normal and disordered voices. Whether one studies the normal or disordered vocal behavior, understanding how the performance effects of behavior influence neural function and structure is critical to the development of optimal treatment strategies that will engender long-term functional restoration of voice when challenged with injury or disease.

UVFP is defined as the loss of mobility of one vocal fold because of injury and is most often attributed to peripheral nervous system lesions.[10] It may be caused by damage to the vagus nerve or one of its branches, the recurrent laryngeal nerve (RLN) or the superior laryngeal nerve (SLN).[11] Voice quality resulting from UVFP is often characterized by various degrees

Accepted for publication July 8, 2010.

From the *Department of Rehabilitation Sciences, College of Health Sciences, University of Kentucky, Lexington, Kentucky; †Department of Behavioral Sciences, College of Medicine, University of Kentucky, Lexington, Kentucky; and the ‡Department of Surgery, College of Medicine, University of Kentucky, Lexington, Kentucky.

Address correspondence and reprint requests to Richard D. Andreatta, Department of Rehabilitation Sciences, College of Health Sciences, University of Kentucky, 900 S. Limestone, Wethington 120-F, Lexington, KY 40536-0200. E-mail: richard.andreatta@uky.edu

Journal of Voice, Vol. 25, No. 2, pp. e53-e59
0892-1997/$36.00

doi:10.1016/j.jvoice.2010.07.002

of hoarseness and significant increases in voice production effort. Treatment for UVFP typically entails surgical and/or behavioral management.[12]

The application of different forms of anesthesia has been used to simulate peripheral neural damage to assess the input- or output-related changes in cortical mappings in animal models[13] and in humans[14] (most often, the digits). These studies have found that during anesthesia, there is an areal increase in the representation of the intact body segment within the cortical representation zone of the anesthetized segment. Cortical mapping changes have been observed within a few minutes after anesthesia inducement.[15,16] On recovery, cortical representations have been observed to return to their original mapping, requiring a time course of a few minutes to hours for complete restoration.[13,14]

The input-dependent shifts in cortical activity during and after peripheral nerve blockade are suggested to be indicative of a latent anatomical network whose influence is revealed when dominant inputs are temporarily blocked. Projections from the thalamus to the cortex (thalamocortical) are known to have overlapping dendrite branching patterns that cross over representational boundaries of neighboring somatosensory zones in cortex. Observed changes to the size and form of central representations rely on the capacity to dynamically shift the balance of excitatory and inhibitory activity within and across representational boundaries, as afforded by the underlying anatomical and functional usage.[17]

Injecting the RLN with a nerve block solution of lidocaine HCL with epinephrine induces a temporary UVFP. In the 1970s and early 1980s, this procedure was routinely used clinically in patients with adductor spasmodic dysphonia (ADSD) to evaluate patient candidacy for nerve sectioning as a treatment for ADSD[18–21] and was first described by Dedo[18] in 1976. More recently, this procedure has been used to experimentally induce vocal fold paralysis to study muscle tension dysphonia and the results of SLN paralysis.[21,22] The present study is the first to use nerve block to temporarily induce UVFP to study the immediate cortical neuroplastic responses to a loss and subsequent recovery of vocal function. This experimental model allows the participant to act as his or her own control, because baseline measures can be obtained before the inducement of the UVFP. It is rarely, if ever, possible to obtain baseline measures in patients with UVFP. Consequently, the current model provides us with a unique opportunity to compare the immediate neuroplastic changes that occur after inducement of UVFP and during recovery from paralysis.

The purpose of this exploratory study was to use fMRI to characterize the central representation of the larynx at three time points: before an induced paralysis, during induced paralysis, and after recovery, within a single participant. This experimental model was used to demonstrate the form and time course of brain activity changes before paralysis, during paralysis, and on recovery. We hypothesized a decrease in activity in the sensorimotor regions during paralysis, with a return of activity levels similar to that observed during the preparalysis phase.

METHODS

Participant

A 57-year-old right-handed male participant with normal voice quality was recruited to test the model of using a temporary induced UVFP (iUVFP) to further our understanding of immediate short-term cortical changes. The study protocol was approved by the Institutional Review Board at the University of Kentucky. The participant signed a written consent form. The participant's normal voice quality was confirmed by perceptual evaluation, patient's self-report, and videostroboscopic examination, revealing normal appearance and function of the glottis. After an initial baseline fMRI scan, right vocal fold paralysis was induced using a 0.3-cc solution of lidocaine and epinephrine (1:100 000) delivered to the right RLN by a board-certified otolaryngologist. The presence of vocal fold paralysis was visually confirmed with a videostroboscopic examination (Figure 1) and through the perceptual presence of a severely hoarse vocal quality. After confirmation of paralysis, a second fMRI scan was then performed during the induced paralysis phase. One hour after recovery from the induced paralysis, as confirmed by a return to normal voice quality and a normal videostroboscopic examination, a third fMRI scan was performed using the same scanning protocol as in the previous two imaging sessions. Preinjection, postinjection, and postrecovery videostroboscopic examinations were performed using a Kay Elemetrics (Montclair, NJ) Rhino-Laryngeal Stroboscope (model RLS 9100 B) with a Kay Elemetrics 70° rigid endoscope (model SN 1541).

Functional magnetic resonance imaging paradigm and task performance

An event-related sparse sampling design was used to obtain fMRI data from the participant. The participant was instructed in a sentence-reading task that included the production of multiple trials of six phonetically balanced sentences from the *Consensus Auditory-Perceptual Evaluation of Voice* (*CAPE-V*; American Speech-Language-Hearing Association, Rockville, MD).[23,24] Two-sentence runs comprising a total of 60 trials of the sentence-production task were used during each functional scan. The instruction and stimuli were displayed onto a screen using commercially available software (*E-Prime*; Psychology Software Tools Inc., Pittsburgh, PA) and an MRI-compatible projection system (SilentVision SV-6011 LCD, Avotec Inc., Stuart, FL). The participant received instructions for each of the tasks projected onto a mirror attached to the head coil. A screen providing the instruction for the task to follow was presented for 3 seconds. The next screen provided the target stimulus, and the participant was instructed to produce the sentences displayed (eg, "Peter will keep at the peak") at a steady pace and at a comfortable loudness. The task time was jittered from 3.5 to 4.5 seconds to ensure capture of the hemodynamic response peak (Figure 2). The delayed latency of the hemodynamic response during the task allowed for an efficient use of an event-related design. The sentences within each run were pseudorandomized.

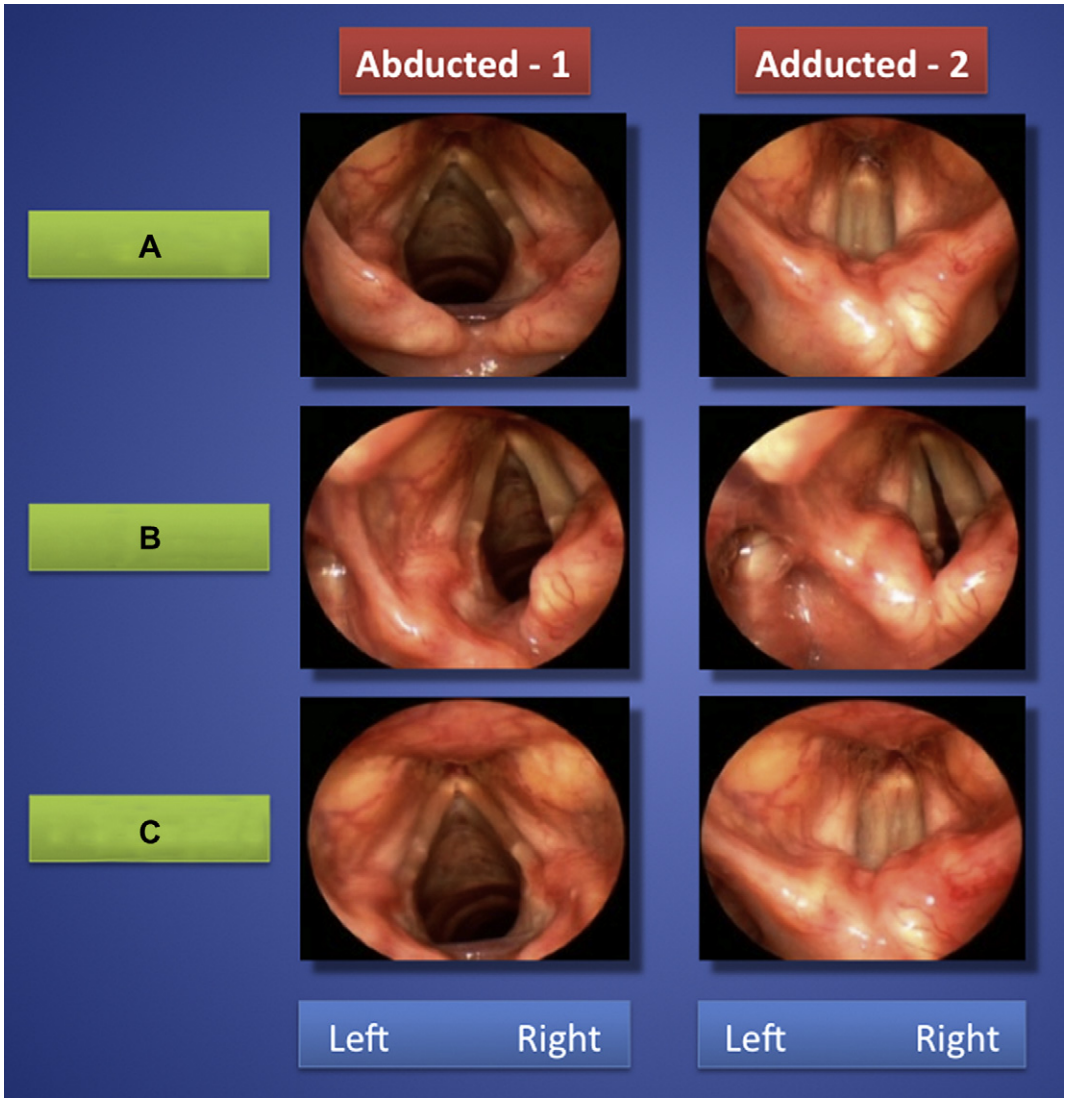

FIGURE 1. Videostroboscopic stills of fully abducted (1) and fully adducted (2) stages when phonating. Vocal folds at baseline (**A**), during paralysis (**B**), and after recovery (**C**) of paralysis. A large glottal gap in panel 2**B** demonstrates the presence of right vocal fold paralysis.

Image acquisition

Structural and fMRI data were acquired on a Siemens Magnetom TRIO 3-Tesla MRI (Siemens USA, Malvern, PA) scanner located in the Magnetic Resonance Imaging and Spectroscopy Center at the University of Kentucky. Two steps were taken to decrease the influence of movement artifact during signal acquisition: (1) participants' heads were stabilized using foam padding between the head and the head coil and (2) an event-related sparse sampling approach was used, wherein the scanner gradients were turned on during the first 3 seconds of instructions to obtain a whole-brain volumetric scan of the blood oxygenation level-dependent (BOLD) activity during the previous task performance. The scanner was turned off during the next 3.5—4.5 seconds during speech production, thus minimizing motion and acoustic contamination during data acquisition.[25] The actual extent of head motion was not calculated during this study. In fact, the sparse-sampling approach used in our investigation ensures that behavior-related motion effects do not negatively impact the fidelity of the fMRI data. Because the speech task is not performed during BOLD acquisition, any movement related to the speech task that could degrade the fMRI signal is absent. The functional images were T2*-weighted echo-planar images. A single echo-planar imaging volume was acquired with time to repeat (TR) = 7.0 seconds. A high-resolution, three-dimensional (3D), anatomical image

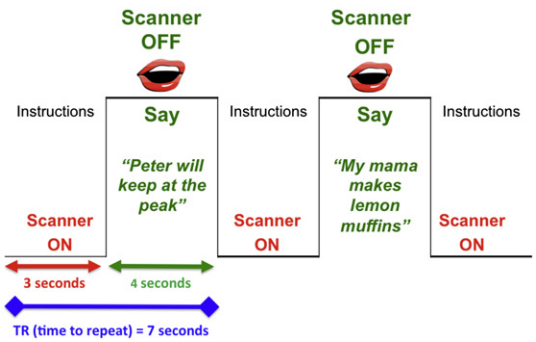

FIGURE 2. Event-related sparse sampling study paradigm.

was acquired using a sagittal T1-weighted (magnetization prepared rapid acquisition gradient echo) sequence (TR = 2100 milliseconds, echo time [TE] = 2.93 milliseconds, inversion time [TI] = 1100 milliseconds, flip angle = 12°, field of view [FOV] = 192 × 224 × 256 mm, with 1 mm [isotropic voxels]). The following parameters were applied: TR = 2.5 seconds; target population [TP] = 156; TE = 30 milliseconds; flip angle = 81°; 39 axial slices; 224 × 224-mm FOV; slice thickness = 3.5 mm; 64 × 64 matrix (yielding 3.5 × 3.5 × 3.5-mm voxel size); and bandwidth = 2056 Hz/pixel.

Data analyses

Image processing and analyses were conducted using the *Analysis of Functional Neuroimages* (*AFNI*; R.W. Cox, National Institute of Health, Bethesda, MD) software package.[26] After preprocessing, the structural 3D data were transformed into *Talairach* space using *AFNI*.[26] The first few functional volumes were eliminated because of T1 saturation effects and differences in timing between slices because of acquisition order and sync interpolation. The fMRI data were motion corrected to the image obtained nearest in time to the structural image and were smoothed (4-mm full-width at half maximum [FWHM]). The general linear model on event-related fMRI was used to estimate the evoked hemodynamic delay for each trial type with no assumptions about the shape of the BOLD responses. The regions of interest, such as the primary sensory cortex (BA 3), primary motor cortex (BA 4), and the cerebellum, were defined anatomically using *AFNI* software.

We calculated the combined fMRI responses in the brain during the sentence task conditions within the subject ($P < 0.05$). The brain regions showing clusters of two or more contiguous voxels were defined as our units of analysis for the overall experimental effect. The extent of BOLD activity presented in Figure 3 reflects overall task-related effect within each phase of the experimental procedure at a statistical threshold of $P < 0.05$. Between-condition comparisons for the differing effects on BOLD activity were not examined at this time. Given that our data are based on an N = 1, there were not sufficient contiguous voxels to adequately perform between-condition comparisons in all three phases. Future investigations with greater numbers of participants will incorporate this level of analysis.

RESULTS

Qualitatively, greater activation was observed during the recovery phase within several brain regions than that at baseline or during UVFP. Table 1 provides the cortical areas activated at the $P < 0.05$ level and the volume of these areas (indicative of

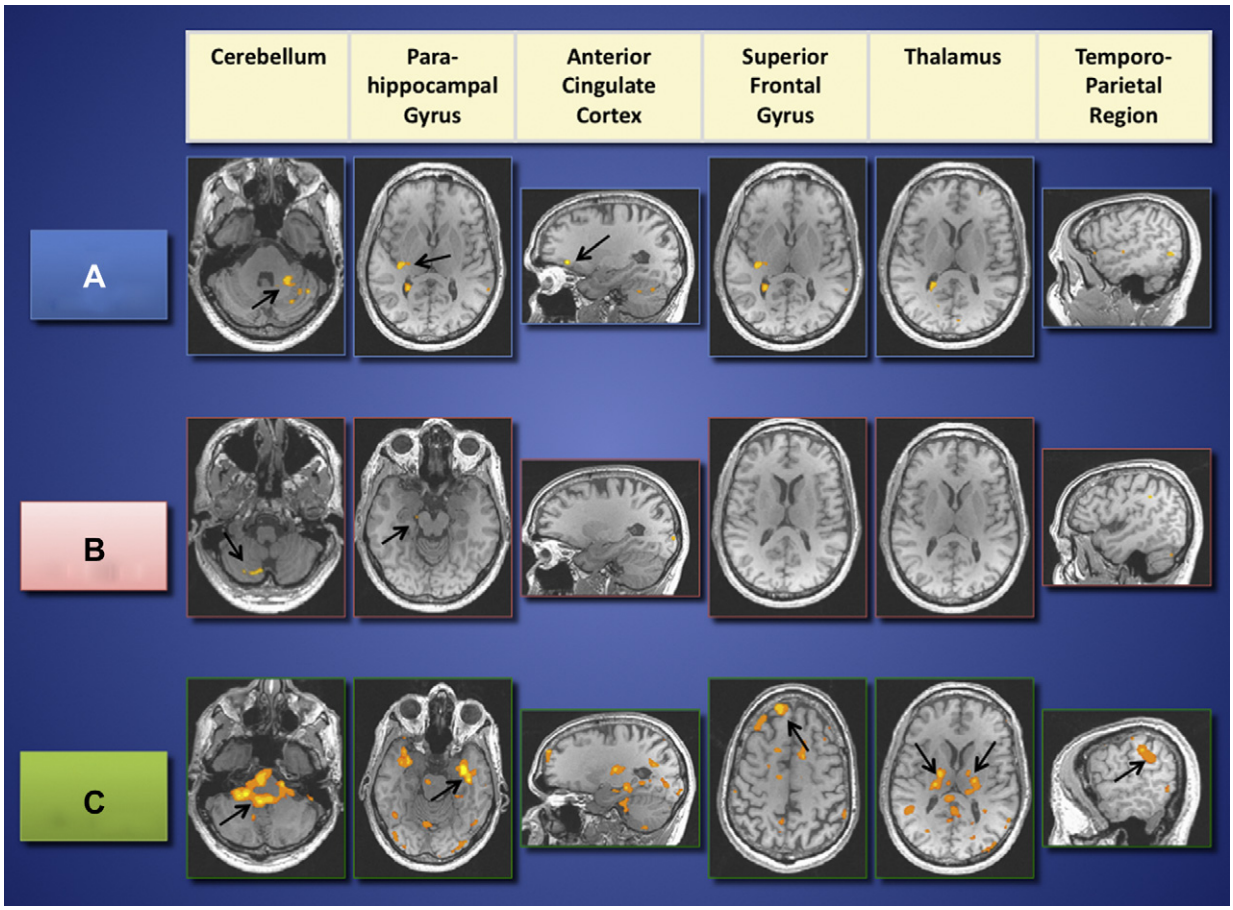

FIGURE 3. fMRI BOLD signals at baseline (**A**), during paralysis (**B**), and after recovery (**C**) of paralysis for selected regions of interest. Specific regions of activation are marked by *an arrow*.

TABLE 1.
***Talaraich* and MNI Coordinates of Brain Regions and Volume of BOLD Responses ($P < 0.05$)**

Phase	Brain Regions	Brodmann Areas	L/R	Coordinates						Volume (mm^3)
				Talaraich			MNI			
				X	Y	Z	X	Y	Z	
Baseline	Anterior cingulate cortex	24	L	−20	34	3	−20	35	5	45
	Inferior frontal gyrus	47	L	−35	20	−5	−35	21	−5	41
During paralysis	No significant activation seen at $P < 0.05$									
Recovery	Parahippocampal gyrus	27	L	−11	−34	2	−11	−35	0	956
	Parahippocampal gyrus	38	L	−32	−5	−17	−32	−4	−21	946
	Superior frontal gyrus	9	L	−6	64	34	−6	64	40	526
	Superior frontal gyrus	8	R	17	49	51	17	48	58	393
	Thalamus (VLN)	—	R	21	−15	9	21	−16	9	446
	Middle temporal gyrus	39	L	−30	−60	20	−30	−63	18	340
	Superior temporal gyrus	38	R	34	3	−20	34	4	−24	311
	Superior temporal gyrus	38	L	−34	21	−29	−34	23	−33	184
	Temporoparietal region	40	R	61	−42	36	62	−45	37	209
	Temporoparietal region	40	R	36	−51	33	36	−54	33	152
	Inferior temporal gyrus	37	L	−54	−60	−9	−55	−61	−14	204
	Medial frontal gyrus	8	L	−44	35	39	−44	34	44	161
	Declive	—	R	40	−63	−22	40	−64	−30	152
	Inferior occipital gyrus	18	R	46	−81	−8	46	−83	−14	126
	Middle temporal gyrus	39	R	33	−68	23	33	−71	21	74
	Middle temporal gyrus	39	L	−47	−76	24	−47	−79	22	64
	Pulvinar	—	R	8	−33	12	−8	−35	11	56
	Precentral gyrus	4	R	42	−6	24	42	−7	26	49
	Superior temporal gyrus	22	L	−54	15	9	−55	15	11	48
	Medial frontal gyrus	6	R	−12	13	51	−12	−13	51	48

Abbreviations: L, left; R, right; VLN, ventrolateral nucleus.

the extent of the activation) for both *Talairach* and Montreal Neuroimaging Institute (MNI) brain area identification systems. Good correspondence between the *Talairach* and MNI system is noted in Table 1, confirming our identification of brain regions. On recovery, a larger volume of fMRI responses was seen within the parahippocampus, superior frontal gyrus, and thalamus, among other areas. A total of 16 regions were identified at an activation threshold of $P < 0.05$ within the recovery phases compared with only two regions at baseline and none during the paralysis phase with an activation greater than 1 voxel. At baseline, both activation sites were located in the left hemisphere. On recovery, greater bilateral representation was observed, especially in the temporal lobe. Left hemisphere dominance was observed for the parahippocampal gyrus and thalamus, whereas the primary motor cortex (precentral gyrus) was activated in the right hemisphere.

BOLD responses in the temporoparietal region were reduced during the paralysis and then increased during the recovery phase. Maximum activation was observed during recovery, as compared with the baseline and the paralysis phases. Our preliminary results indicated overall reduced activity in sensorimotor regions during paralysis (Figure 3B). Recovery from paralysis led to augmented responses, particularly in sensory and association areas (Figure 3C). Finally, there appears to be a distinct pattern of cerebellar activation across the three phases of our perturbation. Greater activation was present in the left cerebellum at baseline but in the right cerebellum during the paralysis, with an apparent shift to midline activation during the recovery phase.

DISCUSSION

As suggested by recent models of speech production and perception,[27,28] the integration of feedback arising from the consequences of normal speech production with predictive feed-forward signals likely includes recursive activity within neural networks located within the left frontal operculum, primary sensorimotor cortices, sensory association areas, and the cerebellum. Balancing feedback and feed-forward processes at any moment in time during behavior is deemed necessary to allow for adaptive changes in the central nervous system when challenged with an external perturbation, such as our iUVFP protocol.[29]

It is reasonable to suggest that a change in functional state of the laryngeal system occurring from the transient paralysis of a vocal fold likely shifted the balance of activity among neural regions involved in feedback and feed-forward processing. This notion is supported by the different patterns of brain activity

observed in our participant from pre- to postinducement of paralysis. For example, before paralysis, cerebellar activity was noted in the left lobe of the cerebellum, with a subsequent shift to the right lobe during the paralysis. The shift in cerebellar activity during the paralysis may have been related to compensatory action of the intact left vocal fold in an effort to decrease the glottal gap secondary to the induced paralysis. During recovery from paralysis, high levels of midline cerebellar activation are consistent with this region's topographic mapping onto the face and vocal tract.[30–33]

The rapid time course of change in auditory and somatosensory feedback produced from a severely hoarse voice during the paralysis to a normal voice quality on recovery may have functioned to heighten activity within the midline cerebellum, because this region is involved in online control of vocalization through an auditory-motor interface.[34–36] The cerebellar activity modifications taken together with the activation changes in the other cortical areas, noted in Figure 3, postinjection, may represent recovery-related phenomena associated with recalibration of the vocalization system after return of function. Although only conjecture at this point, we suspect that if we had waited longer than 1 hour after recovery, the brain responses would have "settled" back to their preparalysis baseline level.

Experimental deafferentation or paralysis of the hand sensorimotor system in animal models and humans has been shown to produce areal expansions and/or increased responsiveness of primary sensorimotor areas.[13–16] In contrast, our functional results indicated decreased cortical activity in primary sensorimotor areas during iUVFP. Although seemingly at odds with findings in limb and hand sensorimotor systems, there are certain methodological and performance factors that may account for this discrepancy. For example, although our perturbation involved the application of an injectable nerve block to achieve paralysis of the vocal fold, reports in the hand have used amputation, nerve transection, crush, and/or ischemia to achieve a peripheral change. Perturbations involving these approaches necessarily affect both motor and sensory capacities. In contrast, our approach only produced a motor deficit of the vocal fold, leaving the sensorium of the larynx intact and responsive. It is likely then that our perturbation, although deleterious to voicing, was not as catastrophic a change when compared with amputation, transection, and ischemic methods. Differences in the magnitude, spatial extent, and the method of perturbation may underlie the noted differences between our results and the cortical changes noted from limb system reports.

CONCLUSIONS

This case study is a preliminary demonstration of the immediate brain responses to an induced and fictive paralysis of the larynx and subsequent recovery. Abrupt changes were observed after inducement of the paralysis, providing evidence of immediate neuroplastic changes that are in keeping with previous literature on activity-dependent reorganization and the effects of deafferentation or paralysis of the limb or digit.[13,14] Clearly, a larger sample size is needed to make any substantive conclusions and achieve a better understanding of the dynamics of this perturbation model. The experimental paralysis model used in this study, though, did allow us to obtain baseline information before the induced dysfunction, a situation that is nearly impossible to obtain in the real-world clinical setting. The presence of this baseline data helped to demonstrate that immediate neuroplastic changes do occur on recovery and that activation is qualitatively different compared with paralysis. However, contrary to our original hypothesis, this pattern was not similar to that seen during baseline. Future research considerations should consider performing an fMRI scan after a longer latency from the initiation of recovery to assess if brain activity does truly "settle" back to baseline over time.

The current model demonstrated short-term plasticity because of an iUVFP and provides evidentiary support for the occurrence of immediate neuroplastic changes within minutes of a functional perturbation. Long-term plastic changes occurring from chronic UVFP in the patient population may very well have substantially different reorganizational patterns, and it will be important to examine cortical response changes in this population. Admittedly, iUVFP is different from pathological and chronic UVFP, but the intent of our model was to provide us with a first-order approximation of the changes that are likely to occur from a premorbid state to a condition where a functional disorder is readily apparent to one where voice has been restored.

The core value of this case report is in the establishment of a strategy to develop a comprehensive accounting of specific neural biomarkers related to long-term functional restoration of voice when challenged by injury or disease. Such a strategy will provide foundational knowledge, permitting the development of hypotheses-driven questions with the goals of better understanding voice disorders and treatments with (1) different origins (central or periphery etiologies), (2) differing treatment paradigms (surgical vs behavioral), and (3) unique time courses for onset and recovery (immediate vs gradual). An important outcome of future investigations using the approach described in this report may be to help identify which traditional behavioral measures best reflect the neural adaptations that are observed during onset and recovery of the induced dysphonia. A reliable understanding between brain-imaging data and behavioral methods may foster a deeper and more complete understanding of pathophysiological models for a variety of voice disorders manifesting primarily in chronic dysphonia.

In essence, our experimental model allowed for a controlled and replicable way to observe the neural events that take place surrounding the onset and resolution of peripherally related vocal deficit, within an extremely compressed time scale. Given the limited ways in which the larynx can be experimentally perturbed, we suggest that iUVFP stands as an effective means to model the task-related neural consequences of dysphonia in humans. Understanding how the performance effects of behavior influence neural function and structure is critical to develop optimal treatment strategies that will engender long-term functional restoration of the voice.

Acknowledgments

The authors thank Dr. David Powell for technical support and training in MRI methodology. This study was funded through a seed grant awarded through the Office of Research, College of Health Sciences, University of Kentucky.

REFERENCES

1. Haslinger B, Erhard P, Dresel C, Castrop F, Roettinger M, Ceballos-Baumann AO. "Silent event-related" fMRI reveals reduced sensorimotor activation in laryngeal dystonia. *Neurology.* 2005;65:1562−1569.
2. Huang J, Francis AP, Carr TH. Studying overt word reading and speech production with event-related fMRI: a method for detecting, assessing, and correcting articulation-induced signal changes and for measuring onset time and duration of articulation. *Brain Lang*. 2008;104:10−23.
3. Loucks TM, Poletto CJ, Simonyan K, Reynolds CL, Ludlow CL. Human brain activation during phonation and exhalation: common volitional control for two upper airway functions. *Neuroimage*. 2007;36:131−143.
4. Ozdemir E, Norton A, Schlaug G. Shared and distinct neural correlates of singing and speaking. *Neuroimage*. 2006;33:628−635.
5. Liotti M, Ramig LO, Vogel D, et al. Hypophonia in Parkinson's disease: neural correlates of voice treatment revealed by PET. *Neurology.* 2003; 60:432−440.
6. Ali SO, Thomassen M, Schulz GM, et al. Alterations in CNS activity induced by botulinum toxin treatment in spasmodic dysphonia: an H215O PET study. *J Speech Lang Hear Res*. 2006;49:1127−1146.
7. Simonyan K, Ludlow CL. Abnormal activation of the primary somatosensory cortex in spasmodic dysphonia: an fMRI study. *Cereb Cortex* 2010. epub ahead of print.
8. Simonyan K, Tovar-Moll F, Ostuni J, et al. Focal white matter changes in spasmodic dysphonia: a combined diffusion tensor imaging and neuropathological study. *Brain*. 2008;131(Pt 2):447−459.
9. Galgano JF, Peck KK, Branski RC, et al. Correlation between functional MRI and voice improvement following type I thyroplasty in unilateral vocal fold paralysis—a case study. *J Voice*. 2009;23:639−645.
10. Benninger MS, Crumley RL, Ford CN, et al. Evaluation and treatment of the unilateral paralyzed vocal fold. *Otolaryngol Head Neck Surg*. 1994; 111:497−508.
11. Kelchner LN, Stemple JC, Gerdeman E, Le Borgne W, Adam S. Etiology, pathophysiology, treatment choices, and voice results for unilateral adductor vocal fold paralysis: a 3-year retrospective. *J Voice*. 1999;13:592−601.
12. Karpenko AN, Dworkin JP, Meleca RJ, Stachler RJ. Cymetra injection for unilateral vocal fold paralysis. *Ann Otol Rhinol Laryngol*. 2003;112: 927−934.
13. Calford MB, Tweedale R. Immediate expansion of receptive fields of neurons in area 3b of macaque monkeys after digit denervation. *Somatosens Mot Res*. 1991;8:249−260.
14. Rossini PM, Martino G, Narici L, et al. Short-term brain "plasticity" in humans: transient finger representation changes in sensory cortex somatotopy following ischemic anesthesia. *Brain Res*. 1994;642:169−177.
15. Brasil-Neto JP, Cohen LG, Pascual-Leone A, Jabir FK, Wall RT, Hallett M. Rapid reversible modulation of human motor outputs after transient deafferentation of the forearm: a study with transcranial magnetic stimulation. *Neurology.* 1992;42:1302−1306.
16. Brasil-Neto JP, Valls-Sole J, Pascual-Leone A, et al. Rapid modulation of human cortical motor outputs following ischaemic nerve block. *Brain*. 1993;116(Pt 3):511−525.
17. Wall JT, Xu J, Wang X. Human brain plasticity: an emerging view of the multiple substrates and mechanisms that cause cortical changes and related sensory dysfunctions after injuries of sensory inputs from the body. *Brain Res Brain Res Rev.* 2002;39:181−215.
18. Dedo HH. Recurrent laryngeal nerve section for spastic dysphonia. *Ann Otol Rhinol Laryngol*. 1976;85(4 Pt 1):451−459.
19. Izdebski K, Shipp T, Dedo HH. Predicting postoperative voice characteristics of spastic dysphonia patients. *Otolaryngol Head Neck Surg*. 1979;87: 428−434.
20. Ludlow CL, Naunton RF, Bassich CJ. Procedures for the selection of spastic dysphonia patients for recurrent laryngeal nerve section. *Otolaryngol Head Neck Surg*. 1984;92:24−31.
21. Smith ME, Roy N, Wilson C. Lidocaine block of the recurrent laryngeal nerve in adductor spasmodic dysphonia: a multidimensional assessment. *Laryngoscope*. 2006;116:591−595.
22. Roy N, Smith ME, Dromey C, Redd J, Neff S, Grennan D. Exploring the phonatory effects of external superior laryngeal nerve paralysis: an in vivo model. *Laryngoscope*. 2009;119:816−826.
23. ASHA. Cape-V scoring form. Available at: http://www.asha.org/uploadedFiles/slp/healthcare/AATVoiceEvaluation.pdf. Accessed August 3, 2010.
24. ASHA. Consensus auditory-perceptual evaluation of voice (CAPE-V)—purpose and applications. Available at: http://www.asha.org/uploadedFiles/members/divs/D3CAPEVprocedures.pdf. Accessed August 3, 2010.
25. Birn R, Bandettini P, Cox R, Shaker R. Event-related fMRI of tasks involving brief motion. *Hum Brain Mapp*. 1999;7:106−114.
26. Cox RW. AFNI: software for analysis and visualization of functional magnetic resonance neuroimages. *Comput Biomed Res*. 1996;29: 162−173.
27. Guenther FH. Cortical interactions underlying the production of speech sounds. *J Commun Disord*. 2006;39:350−365.
28. Guenther FH, Ghosh SS, Tourville JA. Neural modeling and imaging of the cortical interactions underlying syllable production. *Brain Lang*. 2006;96: 280−301.
29. Ghez, C, Krakuer J. In: Kandel E, Schwartz J, Jessell T, eds. Principles of Neural Science. (4th ed). Chapter 33. The organization of movement. 653−673. The McGraw-Hill Companies, Inc.; New York 2000.
30. Ackermann H, Vogel M, Petersen D, Poremba M. Speech deficits in ischaemic cerebellar lesions. *J Neurol*. 1992;239:223−227.
31. Ghosh S. *Understanding cortical and cerebellar contributions to speech production through modeling and functional imaging* [dissertation]. Boston, MA: Boston University; 2005.
32. Riecker A, Ackermann H, Wildgruber D, Dogil G, Grodd W. Opposite hemispheric lateralization effects during speaking and singing at motor cortex, insula and cerebellum. *Neuroreport*. 2000;11:1997−2000.
33. Riecker A, Wildgruber D, Grodd W, Ackermann H. Reorganization of speech production at the motor cortex and cerebellum following capsular infarction: a follow-up functional magnetic resonance imaging study. *Neurocase*. 2002;8:417−423.
34. Martin GF, Beattie MS, Hughes HC, Linauts M, Panneton M. The organization of reticulo-olivo-cerebellar circuits in the North American opossum. *Brain Res*. 1977;137:253−266.
35. Penhune VB, Zattore RJ, Evans AC. Cerebellar contributions to motor timing: a PET study of auditory and visual rhythm reproduction. *J Cogn Neurosci*. 1998;10:752−765.
36. Schulz GM, Varga M, Jeffires K, Ludlow CL, Braun AR. Functional neuroanatomy of human vocalization: an H215O PET study. *Cereb Cortex*. 2005;15:1835−1847.